JOURNAL OF Materials CHEMISTRY

New superconducting charge-transfer salts (BEDT-TTF)$_4$[A·M(C$_2$O$_4$)$_3$]·C$_6$H$_5$NO$_2$ (A = H$_3$O or NH$_4$, M = Cr or Fe, BEDT-TTF = bis(ethylenedithio)tetrathiafulvalene)

Samina Rashid,[a] Scott S. Turner,[a] Peter Day,*[a] Judith A. K. Howard,[b] Philippe Guionneau,[b] Eric J. L. McInnes,[c] Frank E. Mabbs,[c] Robin J. H. Clark,[d] Steven Firth[d] and Tim Biggs[e]

[a]*Davy–Faraday Research Laboratory, The Royal Institution of Great Britain, 21 Albemarle Street, London, UK W1X 4BS. E-mail: pday@ri.ac.uk*
[b]*Department of Chemistry, University of Durham, Durham, UK DH1 3LE*
[c]*Chemistry Department, University of Manchester, Oxford Road, Manchester, UK M13 9PL*
[d]*Christopher Ingold Laboratories, University College, 20 Gordon Street, London, UK WC1H 0AJ*
[e]*Clarendon Laboratory, Oxford, Oxford University, Parks Road, Oxford, UK OX1 3PU*

Received 2nd February 2001, Accepted 13th June 2001
First published as an Advance Article on the web 9th July 2001

The syntheses, crystal structures, and physical properties of two new crystalline charge-transfer salts of BEDT-TTF, bis(ethylenedithio)tetrathiafulvalene, containing tris(oxalato)metallate(III) anions of 3d elements are reported. Electrochemical oxidation of BEDT-TTF in the presence of (NH$_4$)$_3$[Fe(C$_2$O$_4$)$_3$]·3H$_2$O or (NH$_4$)$_3$[Cr(C$_2$O$_4$)$_3$]·3H$_2$O in C$_6$H$_5$NO$_2$, yields crystals of β″-(BEDT-TTF)$_4$[A·Fe(C$_2$O$_4$)$_3$]·C$_6$H$_5$NO$_2$ **[1]** or β″-(BEDT-TTF)$_4$[A·Cr(C$_2$O$_4$)$_3$]·C$_6$H$_5$NO$_2$ **[2]** (A = H$_3$O$^+$ or NH$_4^+$). The crystal structure of **[1]** has been solved at 120 K in the monoclinic space group *C*2/*c*, and that of **[2]** in the same space group at 298 and 120 K. For **[1]**, a = 10.273 Å, b = 19.949 Å, c = 35.030 Å, β = 92.97°, V = 7169.6(2) Å^3, Z = 8. For **[2]**, at 298 K: a = 10.304 Å, b = 20.091 Å, c = 35.251 Å, β = 92.70°, V = 7289.3(2) Å^3, Z = 8, and at 120 K a = 10.283 Å, b = 19.917 Å, c = 34.939 Å, β = 93.30°, V = 7144.4(1) Å^3, Z = 8. The crystal structures of both compounds consist of alternating layers of BEDT-TTF cations and layers containing [M(C$_2$O$_4$)$_3$]$^{3-}$, H$_3$O$^+$ or NH$_4^+$, and PhNO$_2$. The BEDT-TTF molecules are arranged in the β″ packing motif and the tris(oxalato)metallate(III) ions form the well-known honeycomb motif found in many molecular based magnets. SQUID magnetometry, Raman spectroscopy and electron paramagnetic resonance (EPR) measurements were performed on crystals of **[1]**. SQUID magnetometry, single-crystal four-probe conductivity measurements, Raman spectroscopy, EPR and polarised infrared reflectance were performed on crystals of **[2]**. Both compounds have metal to superconducting transitions with T_c = 6.2 K for **[1]** and for **[2]**, T_c = 5.8 K.

Introduction

Charge transfer salts of BEDT-TTF, bis(ethylenedithio)-tetrathiafulvalene, have become a fruitful source of novel collective electronic ground states, including semiconductors,[1] spin–Peierls systems,[2] metals and superconductors.[1,3,4] This variety stems from the way in which the supramolecular organisation of the donors is structured by the size, charge and arrangement of the inorganic anions. In this respect, salts with tris(oxalato)metallate(III) anions have been particularly interesting: they provided the first example of a molecular superconductor containing paramagnetic metal ions and the first superconductor of any kind to contain paramagnetic 3d ions.[3] In addition, the structures and hence properties are extremely sensitive to changes to the solvent molecule included in the lattice. For example, the first BEDT-TTF tris(oxalato)-metallate(III) superconductors, β″-(BEDT-TTF)$_4$[H$_3$O·M(C$_2$O$_4$)$_3$]·PhCN (M = Fe, Cr), with β″ packing mode of the donors, contain PhCN within the hexagonal cavities between the [M(C$_2$O$_4$)$_3$]$^{3-}$. Surprisingly, however, on replacing the included PhCN by C$_5$H$_5$N, phases that exhibit metal–insulator transitions arise.[5] To explore further how change in the solvent molecules included in the crystal modulates the physical properties of this class of compound, we have prepared the corresponding salts containing PhNO$_2$. They are found to be superconductors like the PhCN solvates, but with lower T_c's.

Experimental section

Synthesis and purification of starting materials

Crystals of (NH$_4$)$_3$[M(C$_2$O$_4$)$_3$]·3H$_2$O (M = Fe, Cr), were recrystallised twice from water.[6] BEDT-TTF (Aldrich) was recrystallised from chloroform and 18-crown-6 ether (Aldrich) was purified over CH$_3$CN. Nitrobenzene (Aldrich) was washed with 2 M NaOH, then water, and then 2 M hydrochloric acid followed by water again and dried with MgSO$_4$. Prior to use, the solvent was also fractionally distilled under reduced pressure.

Electrocrystallisation

100 mg of (NH$_4$)$_3$[M(C$_2$O$_4$)$_3$]·3H$_2$O (M = Fe, Cr) was dissolved in 50 cm^3 of nitrobenzene with the aid of 18-crown-6 ether (200 mg). BEDT-TTF (10 mg) was placed in the anode compartment of an H-shaped cell and the remainder was filled with the solution of the tris(oxalato)metallate salt. A constant current of 1 μA was passed across the cell. Small dark, flat needles of β″-(BEDT-TTF)$_4$[A·Fe(C$_2$O$_4$)$_3$]·PhNO$_2$ (A = H$_3$O$^+$ or NH$_4^+$, 6 mg), **[1]**, suitable for X-ray diffraction, were harvested from the platinum anode after three weeks and small, dark-brown flat striated sheets of β″-(BEDT-TTF)$_4$[A·Cr(C$_2$O$_4$)$_3$]·PhNO$_2$ (A = H$_3$O$^+$ or NH$_4^+$, 7 mg), **[2]**, suitable for X-ray diffraction, after two weeks.

DOI: 10.1039/b101134k

Physical measurements

The magnetic susceptibilities of polycrystalline samples of **[1]** and **[2]**, held in gelatine capsules inside a plastic tube, were measured using a Quantum Design MPMS7 SQUID magnetometer. The diamagnetism was estimated as -911.8×10^{-6} cm^3 mol^{-1} for **[1]** and -912.8×10^{-6} cm^3 mol^{-1} for **[2]** from Pascal's constants. Conductivity measurements were performed on an Oxford Instruments Maglab System 2000 in the temperature range 2–300 K, and applied fields from 0 to 7 T. Gold wires (0.0025 mm diam.) were attached to the crystals using Pt paint (Degussa), and the attached wires were connected to an eight-pin integrated circuit plug with Ag paint (RS components). This assembly was fixed onto an IC socket with a 6-way formed pin.

Single crystal X-ray diffraction data were collected using a Bruker Smart CCD diffractometer. The quality of the crystals was first checked at room temperature. In all cases, the strategy was to collect data at θ angle values lower than 28° with a completeness to this value of θ greater than 99.9%. The diffraction frames were integrated using the SAINT package[7] and the intensities corrected for absorption with SADABS[8] while the crystal structures were solved and refined with SHELXTL-Plus.[9]

For **[2]**, separate data were collected at 298 and 120 K using the same crystal. In both cases, the full set of data was collected from four ω-scans (starting at $\omega = -26$, -21, -23, -26° respectively) at values $\phi = 0$, 88, 180, 0° with the detector at $2\theta = -29$° for the three first runs and $+29$° for the last one. At each of these runs, frames (606, 435, 606, 100 respectively) were collected at 0.3° intervals and at 10 seconds per frame. In view of the ambiguity for the monopositive ion it is referred to as A. However, some information concerning this ion is obtained from the infrared and Raman spectra (see below), and its monopositive nature is proven from the charge calculations and Raman reflectivity data. For **[1]**, one data collection was run at 120 K using the same strategy as used previously but with the time exposure of 15 s per frame, the step of 0.2° between two frames, and hence 909, 653, 909, 100 frame collected. All hydrogen atoms for both compounds were placed in idealized positions and refined using the riding model.

Raman spectra of single crystals of **[1]** and **[2]** were measured at room temperature on a Renishaw Raman microscope System 1000 using a He–Ne laser (632.8 nm), a CCD detector, a slit width of 10 μm and 10% neutral density filter. Polarised infrared reflectance spectra of **[2]** were measured using a Bruker IFS 66v interferometer combined with a Nicolet infrared microscope. Data were collected in the range from 800 to 10 000 cm^{-1} using a glowbar, an MCT detector and a KBr beamsplitter in the mid-IR and a tungsten lamp, an InSb detector and a CaF_2 beamsplitter in the near-IR. In both ranges a BaF_2 polariser was used, the spectral resolution being 4 cm^{-1}. Absolute values of reflectance were obtained by comparison with that of a Au mirror placed in the position of the sample. The mismatch between the two ranges of measurement was less than 2%.

The EPR spectra of polycrystalline samples were recorded at X-band (9.5 GHz) and K-band (24 GHz) on a Bruker ESP300E spectrometer with either an ER4102ST, ER6706 or an ER5106 resonator. In the temperature range 290 to 4.2 K, cooling was *via* an Oxford Instruments ESR910 cryostat at X-band, and an ER4118CF cryostat at K-band. Zero-field crossing capabilities allowed sweeping through a range of fields from -40 to $+40$ G in order to study zero-field absorptions.

Results and discussion

Crystal structure

As anticipated, the structures of **[1]** and **[2]** are very closely similar to those of β″-(BEDT-TTF)$_4$[H_3O·Fe(C_2O_4)$_3$]·PhCN in which the BEDT-TTF cations and tris(oxalato)metallate(III) anions are arranged in alternating layers. Table 1 shows the crystallographic data for **[1]** at 120 K and **[2]** at 298 and 120 K respectively. Figs. 1 and 2 show the standard ORTEP diagrams of **[1]** and **[2]** respectively with the atom numbering scheme and 50% thermal ellipsoids. For the purposes of the ORTEP diagrams, the monopositive ion is set as H_3O^+. However, it was difficult to establish crystallographically whether the ion was H_3O^+ or NH_4^+ since the *R* factors showed no significant differences when refined with each alternative (Table 2).

The anionic layers consist of chiral $[M(C_2O_4)_3]^{3-}$ and A^+ ions forming an approximately hexagonal network where successive layers contain either the Δ or Λ forms of the tris(oxalato)metallate(III) anion. The hexagonal cavity is occupied by the solvent molecule $PhNO_2$, which sits in the cavity at a slight angle to the mean plane of the oxalate layer. The cationic layers are formed from BEDT-TTF ions alone which are packed in the β″ arrangement, forming conducting sheets in the *a* and *c* directions. CCDC reference number 157874–157876. See http://www.rsc.org/suppdata/jm/b1/b101134k/ for crystallographic files in .cif format.

Table 1 Crystallographic data for **[1]** at 120(2) K and **[2]** at 298/120 K

Compound	**[1]**	**[2]**	
T/K	120(2)	298(2)	120(2)
Empirical formula	$C_{26}H_{20}Fe_{0.5}N_{0.5}O_{7.5}S_{16}$	$C_{26}H_{20}Cr_{0.5}N_{0.5}O_{7.5}S_{16}$	$C_{26}H_{20}Cr_{0.5}N_{0.5}O_{7.5}S_{16}$
Molecular wt.	998.39	998.39	998.39
Crystal system	Monoclinic	Monoclinic	Monoclinic
Space group	*C*2/*c*	*C*2/*c*	*C*2/*c*
a/Å	10.2732(2)	10.3039(2)	10.2834(1)
b/Å	19.9494(3)	20.0908(3)	19.9172(1)
c/Å*l*)	35.0304(6)	35.2508(4)	34.939(2)
β/deg.	92.969(1)	92.701(1)	93.299(1)
V/Å^3	7169.6(2)	7289.3(2)	7144.4(1)
Z	8	8	8
μ/mm^{-1}	1.207	1.137	1.160
T min, max	0.814, 0.949	0.692, 0.849	0.762, 0.928
Refl. measured	30838	34583	25199
Independent refl.	8238	8365	8179
*R*int(%)	3.5	6.4	4.7
Obs. refl. ($I > 2\sigma(I)$)	6799	4188	5249
Refined parameters	462	460	460
R	0.038	0.065	0.047
*wR*2(F^2)	0.073	0.129	0.088

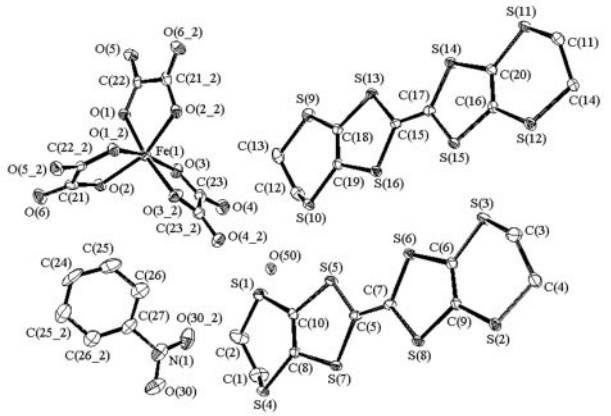

Fig. 1 ORTEP diagram of β″-(BEDT-TTF)$_4$[A·Fe(C_2O_4)$_3$]·$C_6H_5NO_2$ (A = H_3O or NH_4) at 120(2) K.

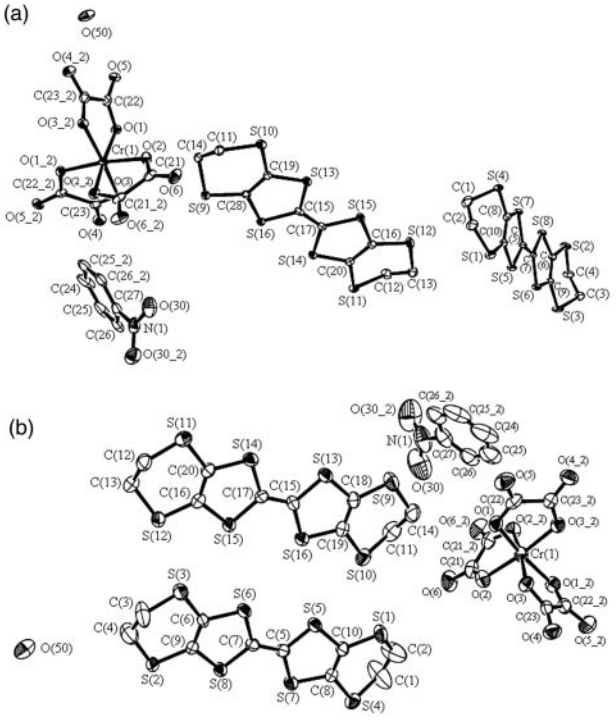

Fig. 2 ORTEP diagram of β″-(BEDT-TTF)$_4$[A·Cr(C_2O_4)$_3$]·$C_6H_5NO_2$ (A = H_3O or NH_4) at (a) 120 K and (b) 298 K.

β″-(BEDT-TTF)$_4$[A·Fe(C_2O_4)$_3$]·$C_6H_5NO_2$, [1] (A = H_3O^+ or NH_4^+)

The asymmetric unit of **[1]** at 120 K contains two crystallographically independent BEDT-TTF molecules. The charge on a BEDT-TTF molecule can be estimated with an accuracy close to 10% using the empirically determined relationship between C–C and C–S bond lengths in the central TTF portion of the molecule.[10] Using this method the BEDT-TTF molecules have similar but not identical positive charges of $+0.6\pm0.1$ and $+0.5\pm0.1$ (Table 3) For both of the independent BEDT-TTF molecules the terminal CH_2–CH_2 groups display the twisted conformation in which one of the carbon atoms is above the central TTF plane and the other is below. The ends of the donor molecules are also eclipsed. There are four short S···S contacts between the BEDT-TTF molecules: S3···S12, 3.31(1) Å, S3···S15, 3.33(1) Å, S5···S10, 3.44(1) Å and S4···S2, between crystallographically identical molecules is 3.39(1) Å. These contacts are slightly longer than those found in the analogous PhCN compound, and indicate that **[1]** should have narrower conduction bands.

Table 2 *R* factors for structural refinements of **[1]** and **[2]** with A = H_3O^+ or NH_4^+

	R		*wR*2	
Compound	A = H_3O^+	A = NH_4^+	A = H_3O^+	A = NH_4^+
[1] at 120 K	0.0380	0.0378	0.0730	0.0724
[2] at 120 K	0.0469	0.0470	0.088	0.0902
[2] at 298 K	0.0652	0.0646	0.129	0.1265

Table 3 Selected bond lengths used to calculate the charge on the BEDT-TTF molecules in **[1]** at 120 K

BEDT-TTF$_A$		BEDT-TTF$_B$	
S16–C15	1.746(3)	S7–C5	1.740(3)
S15–C17	1.745(3)	S5–C5	1.741(3)
S14–C17	1.742(3)	S8–C7	1.734(3)
S14–C20	1.758(3)	S6–C7	1.740(3)
S13–C18	1.755(3)	S7–C8	1.752(3)
S16–C19	1.752(3)	S5–C10	1.755(3)
S15–C16	1.746(3)	S8–C9	1.757(3)
C19–C18	1.350(4)	S6–C6	1.745(3)
C20–C16	1.358(4)	C9–C6	1.355(4)
C17–C15	1.362(4)	C10–C8	1.352(4)
C15–S13	1.743(3)	C7–C5	1.369(3)

The $PhNO_2$ sits in the hexagonal cavity of the anionic layer at an angle of 31.0° to the mean plane of the layer. The CH_2–CH_2 groups of the BEDT-TTF molecules in the organic layer form H-bonds to the O atoms of the $[C_2O_4]^{2-}$ ligands in the inorganic layer, allowing the BEDT-TTF CH_2–CH_2 groups to dock into the anion layer. When compared to the extent of H-bonding between the donor–acceptor layers in the analogous PhCN compound, it is apparent that those in **[1]** are longer. In fact the closest H···O contact in **[1]** is 2.88(2) Å, whereas in the PhCN derivative it is 2.44(1) Å.

β″-(BEDT-TTF)$_4$[A·Cr(C_2O_4)$_3$]·$C_6H_5NO_2$, [2] (A = H_3O^+ or NH_4^+)

As with **[1]** there are two crystallographically independent BEDT-TTF molecules in the unit cell with calculated charges of $+0.7\pm0.1$ and $+0.6\pm0.1$, unchanged on change of temperature from 298 to 120 K (Table 4) In the molecule which contains atoms C15 and C17 the CH_2–CH_2 groups are twisted and eclipsed, as previously defined. However, at 298 K, the CH_2–CH_2 group on one side in the second molecule containing atoms C5 and C7 is twisted, though it retains the boat conformation at the other end. A "boat" conformation results where both CH_2–CH_2 carbon atoms are on the same side of the plane defined by the central TTF portion of the molecule. Torsion angles of the CH_2–CH_2 groups in the crystallographically independent donors, BEDT-TTF$_A$ and BEDT-TTF$_B$ are given in Table 5. The torsion angle is defined as the angle between a plane composed of three atoms (the S atom on the outer ring of BEDT-TTF and the two C atoms of the terminal ethylene group) and a fourth atom (the second S atom on the outer BEDT-TTF ring).

The torsion angles of the twisted conformations are each about 70° whereas that for the boat conformation is considerably smaller. A perfect boat conformation would result in a torsion angle of 0°. It is noteworthy that there is considerably more thermal disorder on the C atoms in the boat CH_2–CH_2 group, as can be seen clearly on C1 and C2 from the 50% thermal ellipsoids for the 298 K structure shown in Fig. 2. The H atoms which are attached to these C atoms are in close contact with the O atom of the $PhNO_2$, which may promote a weak H bonding interaction. Thus the H2A–O30 distance is 2.47(1) Å and the H2B–O30 distance is 2.94(1) Å. This arrangement, in which a quarter of the CH_2–CH_2 groups has

Table 4 Selected bond lengths used to calculate the charge on the BEDT-TTF molecules in **[2]** at 120(2) and 298(2) K

298 K		120 K	
BEDT-TTF_A		BEDT-TTF_A	
S16–C15	1.724(6)	S13–C15	1.739(4)
S13–C15	1.732(6)	S16–C15	1.741(4)
S15–C17	1.741(6)	S15–C17	1.744(4)
S14–C17	1.743(5)	S14–C17	1.746(4)
S14–C20	1.749(6)	S15–C16	1.751(4)
S13–C18	1.752(6)	S14–C20	1.747(4)
S16–C19	1.746(6)	S13–C19	1.755(4)
S15–C16	1.740(6)	S16–C28	1.748(3)
C19–C18	1.346(8)	C21–C20	1.745(4)
C20–C16	1.360(8)	C20–C16	1.363(5)
C17–C15	1.379(7)	C28–C19	1.360(5)
BEDT-TTF_B		BEDT-TTF_B	
S7–C5	1.740(5)	S6–C7	1.739(4)
S5–C5	1.735(6)	S8–C7	1.744(4)
S8–C7	1.733(6)	S5–C5	1.745(4)
S6–C7	1.730(6)	S7–C5	1.74(4)
S7–C8	1.751(6)	S6–C9	1.747(4)
S5–C5	1.735(6)	S8–C6	1.748(4)
S8–C9	1.739(6)	S5–C10	1.75(4)
S6–C6	1.742(5)	S4–C8	1.748(4)
C9–C6	1.342(7)	C5–C7	1.358(5)
C10–C8	1.335(7)	C9–C6	1.359(5)
C7–C5	1.373(7)	C8–C10	1.364(5)

a different conformation from the rest, has been found before in the closely related compound β″-(BEDT-TTF)$_4$[H_3O·Cr-(C_2O_4)$_3$]·C_5H_5N[5] which undergoes a metal–insulator transition at 116 K. The torsion angles for the latter compound are listed for comparison in Table 5. In the C_5H_5N compound, the conformation of the fourth CH_2–CH_2 group remains disordered and does not change with decreasing temperature. However, as can be seen in Table 5, the magnitude of the torsion angle for S1–C2–C1–S4 in **[2]** increases from −23 to −57° on lowering the temperature, indicating that the CH_2–CH_2 group becomes more twisted. This increase in ordering could be the reason for the formation of a superconducting state in **[1]** at a lower temperature, as distinct from the insulating state observed for the C_5H_5N compound.

The angle of the $PhNO_2$ plane (defined by three points on the phenyl ring) was measured with respect to the anion plane (defined by three terminal oxygen atoms on the tris(oxalato)-metallate(III) anion pointing in the *c* direction). This angle is 32.0° at both 298 and 120 K. At 298 K the four shortest S···S distances are S3···S12, 3.34(2) Å, S3···S15, 3.38(1) Å, S5···S10, 3.51(1) Å and S2···S4, 3.42(1) Å, which at 120 K decrease to 3.31(1) Å, 3.34(1) Å, 3.43(1) Å, 3.39(1) Å, respectively. When compared to the analogous PhCN compound the S···S contacts are slightly the longer, suggesting smaller transfer integrals and narrower conduction bands.

The derivation of structure–property relationships requires a detailed analysis of the crystal structures. It is well known that for these compounds minor modifications to the structure can lead to drastic changes in the properties. Analysis is further complicated by the effect of incorporating functionalised anions that are not only different in size but have different localized magnetic moments. The solvent molecule, thought to have a templating effect in stabilizing the structure, is assumed to be inert and therefore exerts an effect by altering the solubility during electrocrystallisation or by determining the size of the hexagonal cavity.

Table 5 Torsion angles on the CH_2–CH_2 groups of the crystallographically independent BEDT-TTF molecules in **[1]**, **[2]** and in β″-(BEDT-TTF)$_4$[H_3O·Fe(C_2O_4)$_3$]·C_5H_5N, **[3]**

Compound	BEDT-TTF_A		BEDT-TTF_B	
[1] at 120 K	S2–C4–C3–S3	−71.0	S12–C14–C11–S11	−69.8
	S4–C1–C2–S1	58.0	S10–C12–C13–S9	70.6
[2] at 120 K	S11–C12–C13–S12	68.9	S2–C4–C3–S3	71.0
	S9–C14–C11–S10	−70.2	S1–C2–C1–S4	−57.2
[2] at 298 K	S9–C14–C11–S10	−70.4	S1–C2–C1–S4	−22.9
	S11–C12–C13–S12	68.1	S2–C4–C3–S3	57.7
[3] at 150 K	−69.7 and 66.9		57.6 and 6.9	

In fact it is the anion that primarily determines the size of the solvent cavity, with the Fe salts having larger cavity volumes than the corresponding Cr ions. Consequently, the solvent molecule plane in the Fe salts is at a smaller angle to the mean plane of the metal tris(oxalato)metallate(III) anions.

The unit cell volumes of **[1]** and **[2]** indicate that their lattices are more loosely packed than those of the analogous PhCN compounds. The greatest difference between the two solvates is in the crystallographic angle β (0.7%), which essentially governs the size of the *bc* plane, the latter being parallel to the BEDT-TTF layer; this difference would therefore determine the extent of overlap of the s orbitals between the BEDT-TTF molecules. There is less overlap in the $PhNO_2$ compounds because the unit cell volume is larger and, as a result of this, they have longer S···S contacts, resulting in reduced conductivity and lower T_c's. So far in this family of compounds, β″-(BEDT-TTF)$_4$[H_3O·Fe(C_2O_4)$_3$]·PhCN has the highest T_c with the shortest S···S contacts of between 3.30 and 3.47 Å, and **[2]** with the lowest T_c, has close contacts of between 3.31(1) and 3.58(1) Å.

The most disordered atoms are those on the terminal CH_2–CH_2 groups of the BEDT-TTF molecules. They adopt different conformations, depending on how they interact with the anion layer. The $PhNO_2$ salts have weaker hydrogen-bonding interactions between the organic and inorganic layers. This "docking" interaction is probably one of the factors accounting for the lower T_c's of the $PhNO_2$ compounds.

Physical properties

Magnetic susceptibility

To detect the Meissner–Oshenfield effect, samples were cooled in zero field and a field of 5 G was applied while measuring the magnetisation while warming to above T_c. The sample was then re-cooled and the magnetisation measured again in the same applied field. This procedure was repeated for increasing fields up to 80 G over the temperature range 2 to 14 K. The magnetic susceptibility was also measured at 10^4 G from 2 to 300 K. For compound **[1]** the susceptibility obeys the Curie–Weiss law above 80 G and has a temperature-independent Pauli contribution of 1×10^{-5} cm^3 mol^{-1}. The fitted Curie constant is 3.877 emu mol^{-1} (4.375 is expected for high spin Fe^{3+})[11] and the Weiss constant is −0.16 K indicating very weak antiferromagnetic interaction between the Fe centres. On cooling the sample in zero applied field and measuring the magnetisation in an applied field of 5 G from 2 to 14 K, the response is diamagnetic below 6.2 K which indicates the onset of superconductivity at this temperature. Type II superconducting behavior was indicated, since the magnetic flux is able to penetrate the sample as the sample is re-cooled in the same applied field (Fig. 3).

Compound **[2]** is also a type II superconductor but has a lower T_c of 5.8 K. At fields above 80 G, superconductivity is completely suppressed, Fig. 4, and Curie–Weiss behaviour is observed with a Curie constant of 2.129 (1.87 is expected for Cr^{3+})[11] and a Weiss constant of −1.44 K indicating weak antiferromagnetic interaction between the Cr centres.

In view of the fact that both Curie constants for **[1]** and **[2]** were slightly different to those expected, the SQUID experiment was repeated on three separate preparations of each compound. This gave identical results as reported above. In the case of **[1]** this indicates some antiferromagnetic interactions. For **[2]** it seems that there must be a small contribution from

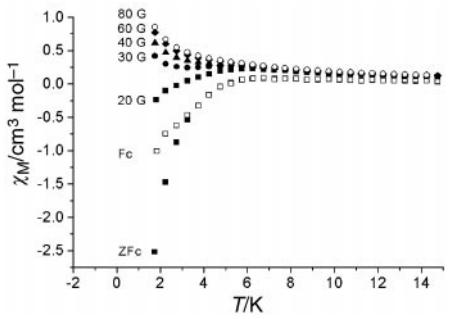

Fig. 3 Temperature dependence of magnetic susceptibility of **[1]** in fields from 0 to 80 G. Zero field cooled (ZFc), field cooled (Fc) plots show the superconducting T_c.

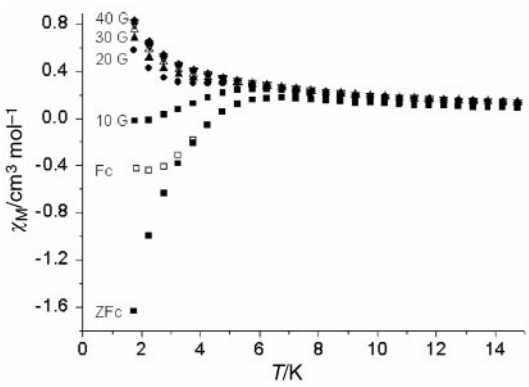

Fig. 4 Temperature dependence of magnetic susceptibility of **[2]** in fields from 0 to 40 G. Zero field cooled (ZFc), field cooled (Fc) plots show the superconducting T_c.

the spin on the BEDT-TTF radicals. It is not clear why these isostructural materials should show slightly different magnetic phenomena.

Electrical conductivity

Single crystals of **[1]** were not suitable for transport measurements due to excessive twinning and the small crystal size. Four probe dc conductivity measurements on single crystals of **[2]** confirm that the compound is superconducting with the onset of the superconducting transition at about 6 K reaching zero resistance at 3.2 K (Fig. 5). The crystals are flat thin rectangular sheets, limiting the measurement of conductivity to that parallel to the *c* axis only. Measurements were made from 31 to 2 K at 1 K steps. On applying a magnetic field the resistance increases as expected, and the superconducting state is completely destroyed at 1000 G. The critical field, H_c, was determined by applying fields from 0 to 1000 G in 10 G intervals and from 1000 to 2×10^4 G in 1000 G intervals at 2 K. The critical field at which the Cooper pairs are disrupted is 300 G, much higher than that obtained from SQUID measurements.

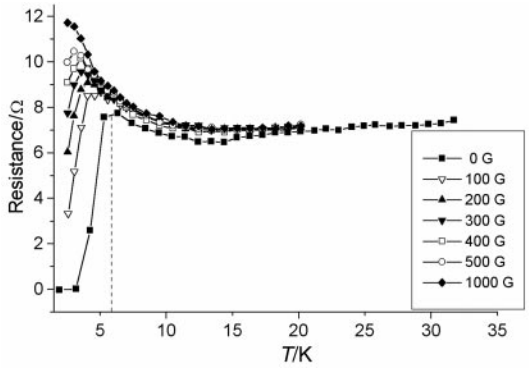

Fig. 5 Magnetoresistance measurements of **[1]** in fields from 0 to 1 T.

Raman spectroscopy

The two totally symmetrical C=C stretching frequencies of BEDT-TTF between 1400 and 1550 cm^{-1} (ν_3 and ν_4) have large electron–phonon coupling constants and so are very sensitive to the charge on the donor molecule. Wang *et al.*[12] showed for related complexes that there is an approximately linear relationship between the degree of charge-transfer and the shift in the wavenumbers of ν_3 and ν_4. From the BEDT-TTF charges calculated for **[1]** from the C–C and C–S bond lengths, the expected Raman band wavenumbers would be 1492 cm^{-1} (ν_3) and 1459 cm^{-1} (ν_4). From the experimental spectrum the two bands attributed to totally symmetrical C=C stretching modes occur at $\nu_3=1495$ cm^{-1} and $\nu_4=1466$ cm^{-1}, corresponding to an approximate charge of +0.51 and +0.48 on the two BEDT-TTF ions in **[1]**. This agrees with the conclusions drawn from the crystal structure (Fig. 6). The charge found on the BEDT-TTF also confirms that the A group is monopositive. The weak band at 1420 cm^{-1} is in the correct place expected for ν_4 of NH_4^+ even though this band would be typically broader. The Raman spectrum of **[2]** shows that $\nu_3=1494.6$ cm^{-1} and $\nu_4=1470.3$ cm^{-1} and corresponds to BEDT-TTF with a charge of +0.48, (Fig. 6). As with compound **[1]**, since the formal charge on the anion is 3− the A group must be monopositive.

Electron paramagnetic resonance

As with other compounds in the same series, both **[1]** and **[2]** exhibit low field microwave absorption (LFMA) signals indicative of superconductivity[13–16] (Figs. 7a and 7b). For **[1]** the LFMA is detected up to 18 K at the K-band frequency and for **[2]** the LFMA is observed below 10 K at X-band and K-band frequencies. Since these temperatures are above the T_c measured by susceptibility, the effect may be due to two-dimensional short-range superconducting fluctuations or surface effects.

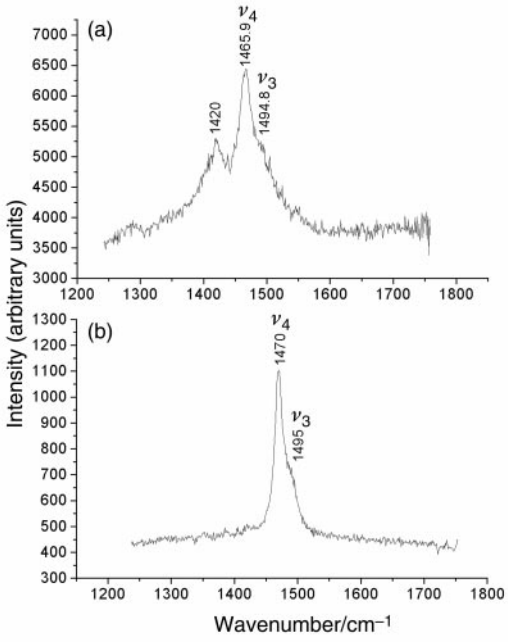

Fig. 6 Room temperature Raman spectra of **[1]** and **[2]** in the range 1200 to 1800 cm^{-1}.

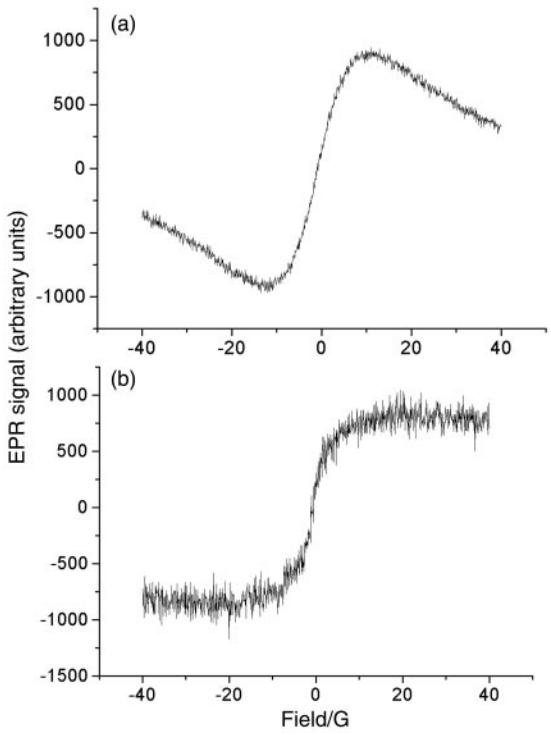

Fig. 7 Low field microwave absorption (LFMA) signals for **[1]**, and **[2]**. Measured at 4.2 K with K-band EPR.

Polarised infrared reflectance

The polarised infrared reflectivity of single crystals of **[2]** at room temperature was measured both parallel and perpendicular to the long axis of the rectangular crystal (Fig. 8). The spectrum is of the form expected for a metal, with high reflectivities, and an approximate threefold difference in reflectance for polarisation of the incident electric vector 0 and 90° to the crystal *c* axis. This indicates that the band structure is highly anisotropic, as expected (the unpolarised spectra are the mean of the 90 and 0° measurements). The frequency dependence of the reflectivity could not be fitted to the simple Drude model, which suggests that a more complex conduction mechanism is in operation. Superimposed on the electronic contribution are peaks close to the vibrational transitions, which can be assigned to fundamentals of the $[Cr(C_2O_4)_3]^{2-}$ ion: *e.g.* the O–C–O asymmetric stretching vibration which occurs at 1655 cm^{-1}. It is noted that there is no strong band about 3050 cm^{-1} for the N–H stretch, which would be expected if **[2]** contained NH_4^+. This, together with the Raman data, may indicate that compound **[1]** crystallises with $A = NH_4^+$ whereas **[2]** has $A = H_3O^+$, although more definitive evidence is required to be certain.

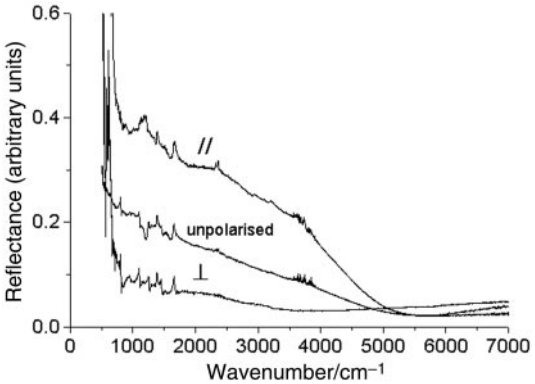

Fig. 8 Polarised infrared reflectance spectra of **[2]** measured parallel (//) and perpendicular (⊥) to the crystallographic *c* axis.

Conclusion

We have synthesised and characterised the crystal structures and physical properties of two new molecular charge transfer salts belonging to the general class β″-(BEDT-TTF)$_4$[A·M-$(C_2O_4)_3$]S, where S is an included solvent molecule. Like the compounds where S = PhCN, but in contrast to those where $S = C_5H_5N$, the new compounds with $S = PhNO_2$ are type II superconductors, though with T_c's and H_c's slightly lower than in the PhCN compounds that contain the same 3d metal ion M. Surprisingly, in view of correlations between increasing unit cell volume and higher T_c for other series of molecular superconductors such as β″-(BEDT-TTF)$_2$X[17,18] (X = I_3, AuI_2, *etc.*) and A_3C_{60}[19] (A = group 1 cation), the lower T_c of the $PhNO_2$ compounds are associated with slightly larger unit cell volumes. Thus at 120 K, for M = Fe, S = PhCN, $V = 7157$ Å^3 while for M = Fe, S = $PhNO_2$, $V = 7169$ Å^3. However, given the very small differences of less than 0.2% in unit cell volumes caution is needed in interpreting these results. Furthermore, intermolecular S···S distances are, on the whole, slightly larger in the $PhNO_2$ compounds than the PhCN ones, suggesting narrower bands and, on a simple BCS view, higher T_c. However, probably a more significant determinant of the collective properties of this series of compounds is the disorder of the terminal CH_2–CH_2 groups of the BEDT-TTF, which is determined by the volume and the H-bonding capabilities of the solvent molecule. It is clear that the lower T_c of the $PhNO_2$ salts is not correlated with one single structural parameter. More salts in this series with different included solvent molecules will need to be examined to identify the critical structural parameters and to classify the supramolecular chemistry of such complex lattices.

Acknowledgements

The UK Engineering and Physical Sciences Research Council and the University of London Intercollegiate Research Service have supported this work. Phillipe Guionneau thanks the European Commission for the award of a Marie Curie Research Fellowship.

References

1 M. Kurmoo, A. W. Graham, P. Day, S. J. Coles, M. B. Hursthouse, J. L. Caulfield, J. Singleton, F. L. Pratt, W. Hayes, L. Ducasse and P. Guionneau, *J. Am. Chem. Soc.*, 1995, **117**, 12209.
2 P. Guionneau, J. Gaultier, M. Rahal, G. Bravic, J. M. Mellado, D. Chasseau, L. Ducasse, M. Kurmoo and P. Day, *J. Mater. Chem.*, 1995, **5**, 1639.
3 A. W. Graham, M. Kurmoo and P. Day, *J. Chem. Soc., Chem. Commun.*, 1995, **20**, 2061.
4 L. Martin, S. S. Turner, P. Day, F. E. Mabbs and E. J. L. McInnes, *Chem. Commun.*, 1997, 1367.
5 S. S. Turner, P. Day, K. M. A. Malik, M. B. Hursthouse, S. J. Teat, E. J. MacLean, L. Martin and S. A. French, *Inorg. Chem.*, 1999, **38**, 3543.
6 J. C. Bailar and E. M. Jones, *Inorg. Synth.*, 1939, **1**, 1993.
7 SAINT Version 4.050, Siemens Analytical X-ray Instruments, Madison, USA, 1995.
8 SADABS Empirical Absorption Program, G. M. Sheldrick University of Göttingen, Germany.
9 SHELXTL-Plus, G. M. Sheldrick, Release 4.1 edn., Siemens Analytical X-ray Instruments Inc., Madison, Wisconsin, USA, 1991.
10 P. Guionneau, C. J. Kepert, G. Bravic, D. Chasseau, M. R. Truter, M. Kurmoo and P. Day, *Synth. Met.*, 1997, **86**, 1973.
11 R. L. Carlin, *Magnetochemistry*, Springer Verlag, Weinheim, 1986.
12 H. H. Wang, J. R. Ferraro, J. M. Williams, U. Geiser and J. A. Schlueter, *J. Chem. Soc., Chem. Commun.*, 1994, **16**, 1893.
13 D. Achkir, M. Poirier, C. Bourbonnais, G. Quiron, C. Lenoir, P. Batail and D. Jerome, *Phys. Rev. B*, 1993, **47**, 11595.
14 A. Dulcic, R. H. Crepeau and J. H. Freed, *Phys. Rev. B*, 1989, **39**, 4249.
15 F. J. Owens, *Phys. C (Amsterdam)*, 1991, **178**, 456.

16 M. J. Rosseinsky, A. P. Ramirez, S. H. Glarum, D. W. Murphy, A. F. Haddon, T. T. M. Palstra, A. R. Kortan, S. M. Zahurak and A. V. Makhija, *Phys. Rev. Lett.*, 1991, **66**, 2830.
17 V. F. Kaminskii, T. G. Prokhorova, R. P. Shibaeva and E. B. Yagubskii, *JETP Lett. Engl. Transl.*, 1984, **39**, 17.
18 H. H. Wang, M. A. Beno, U. Geiser, M. A. Firestone, K. S. Webb, L. Nunez, G. W. Crabtree, K. D. Carlson, J. M. Williams, L. J. Azevedo, J. F. Kwak and J. E. Schirber, *Inorg. Chem.*, 1985, **24**, 2465.
19 M. Baenitz, M. Heinze, K. Luders, H. Werner and R. Schlogl, *Solid State Commun.*, 1994, **91**, 337.